Chiral selectivity of polyglycerol-based amphiphiles incorporating different aromatic cores

A. Setaro [*,1], C.S. Popeney[2], M.U. Witt[1], P. Bluemmel[1], M. Glaeske[1], R. Haag[2], and S. Reich[1]

[1] Department of Physics of the Freie Universität Berlin, Arnimallee 14, 14195 Berlin, Germany

[2] Department of Chemistry and Biochemistry of the Freie Universität Berlin, Takusstrasse 3, 14195 Berlin, Germany

Keywords Carbon nanotubes; Chirality selection; Isolation and solubilisation; Polyglycerol-based surfactants.

Customized polyglycerol-based surfactants incorporating different aromatic cores are used to isolate and suspend carbon nanotubes in water. Different cores yield suspension with distinct chiral species distribution. Increasing the number of the phenyl rings connecting head and tail, the dispersion of the semiconducting species becomes sharper towards the nanotubes with bigger family index.

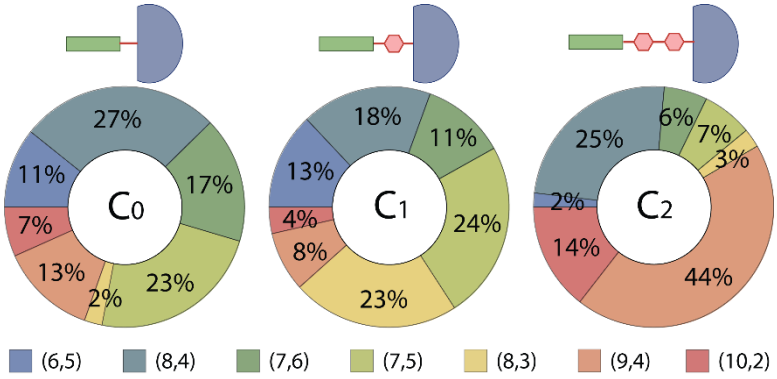

1. Introduction

Carbon nanotubes (CNTs) are hollow cylinders made of pure carbon. Single-walled carbon nanotubes (SWNTs) can be depicted as a portion of a single-layer graphene cut along a certain direction and folded up. The vector describing the length and direction of the cut, the chiral vector

c=(n1,n2), is expressed in terms of the graphene unit cell vectors. Most of the amazing mechanical and electronic properties of SWNTs are inherited from graphene [1]. The additional periodic boundary conditions due to the folding provides SWNTs with their additional peculiar character. Depending upon the chiral vector, SWNTs can be semiconducting or metallic, each chiral species being a different material with its unique and distinctive optoelectronic properties [1]. Their 1-d nature reflects in the structure of their density of states, characterized by the sharp van Hove singularities, whose energetic separation univocally identify a given (n1,n2) species.

Despite their unique character, SWNTs cannot be exploited for extensive and upscalable applications because as-produced SWNTs are chirally polydisperse; the isolation of a targeted single species is still a challenging task. The choice of a smart precursor has recently made it possible to grow nanotubes of the single (6,6) chiral species [2]. The selective growth of an arbitrary targeted chiral species remains technologically unaccessible so far. Single chiralities are sorted out of the polydisperse production batches following different approaches. Density gradient ultracentrifugation [3] and gel dielectrophoresis [4], for example, take advantage, respectively, of the distinct density and mobility of different nanotube species to produce chirally enriched solution. The low production yield of such techniques makes them useful for fundamental studies but unpractical for extensive applications. An alternative approach, producing virtually any amount of targeted chiralities, has been developed by Kataura and co-workers and is based on the overload of multicolumns filled with dextran-based gels [5]. The technique requires several filtration cycles and large amount of materials. Khiripin et al. suggested to take advantage of the spontaneous partition of SWNTs between two immiscible phases obtained by mixing polyethylene glycol and dextran in water [6]. In this way they have been able to separate small- and big-diameter nanotubes and metallic from semiconducting. The separation takes place directly at the solubilization stage and does not require additional steps and tools, making the method easily up-scalable. To take over

the chiral selectivity into this process, selectivity towards specific chiral species has to be enrolled within the solubilization stage. Marquis et al. showed that amphiphiles embodying flat aromatic fragments selectively solubilized carbon nanotubes belonging to specific chiral species [7]. Tu et al. even set up a database of DNA fragments to solubilize targeted semiconducting species [8]. The strong adsorption energy of the wrapped DNA fragments around the SWNTs makes it hard to remove them from the nanotube sidewall, preventing their exploitation where as-pristine, uncovered nanotubes are needed. Isolation and solubilization by en-closing SWNTs in surfactant micelles serves efficiently to this purpose; disruption of the surfactant micelles leaves the tubes uncovered and triggers their reaggregation and precipitation. Dialysis can moreover be employed to easily replace one surfactant with others [7].

Mimicking the structure of the commercially available SDS surfactant, we introduced a new class of amphiphiles that exploited the steric hindrance of polyglycerol dentritic structures to solubilize the tubes rather then the SDS' ionic head [9]. The surfactant comprised a tail made of an alkyl chain, effective in debundling the tubes, and a polyglycerol head, to ensure water solubility. Modifying the head and tail morphology as well as including different aromatic fragments between head and tail, the amphiphiles displayed different properties, such as critical micellar concentration, nanotubes dispersing ability, long-term stability, and so on [10]. Small aromatic moieties, e.g. pyrene, perylene, porphirine, can replace alkyl chain to bring tubes in solution [11-13] but the higher adsorption energy makes the surfactant efficiently stick on the nanotubes and more difficult to be desorbed and removed. The choice of the aromatic core impacts the nanotube-surfactant interaction strength and how efficiently they can be replaced with other surfactants [14,15]. By incorporating an azobenzene-derivative between head and tail, we have even been able to trigger the micelle disruption and nanotube re-aggregation just by exposure of UV light [16].

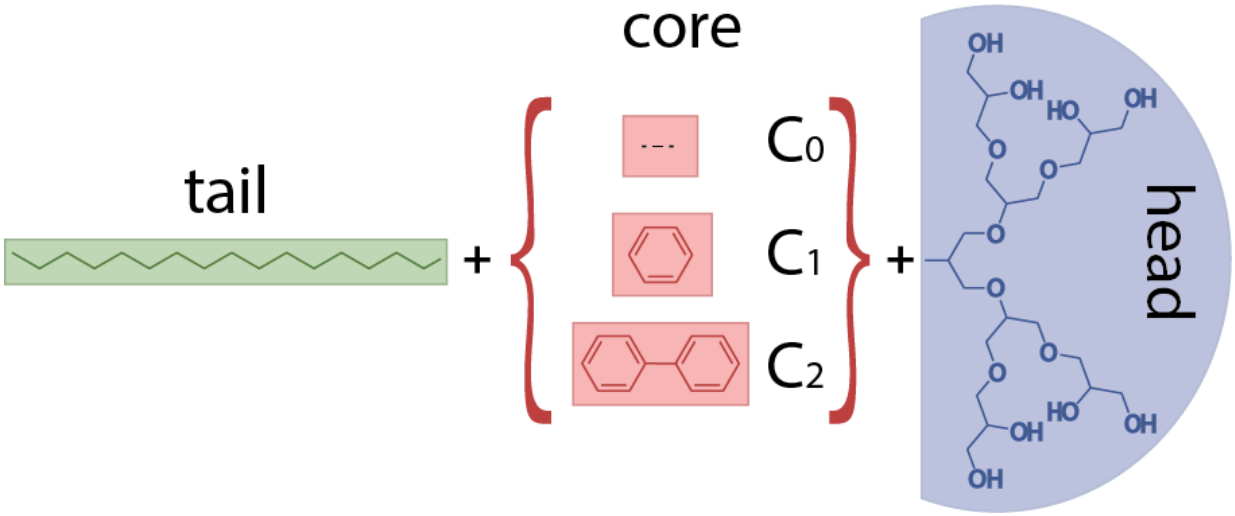

Figure 1 Schematic depiction of the surfactants used in this work.

In this work we will focus on the chiral dispersing ability of three surfactants sharing the same head (polyglycerol dendron) and tail (alkyl chain). For the choice of the core, we compared small aromatic fragments with increasing affinity for the SWNTs sidewall. By comparing the times of flight of several polyaromatic hydrocarbons within a cylinder coated with nanotubes, Yoo et al. established a ranking of the molecule-tube affinity in the noncovalent functionalization scheme [17]. Taking advantage of their retention time experiments, we chose to compare the performances of an amphiphile just made by connecting the alkyl chain to the polyglycerol head (compound C_0), one with a phenyl moiety connecting head an tail (compound C_1), and the last one with a biphenyl fragment connecting head and tail (compound C_2). Figure 1 illustrates the molecular structure of the compounds considered in this work: The alkyl chain tail is green, the aromatic cores are highlighted in red and the polyglycerol head is marked in blue.

Increasing the number of phenyl rings embodied within the amphiphiles core boosts the selectivity of the resulting dispersions towards specific SWNTs species.

2. Experimental setup and sample preparation

To ensure consistency of the comparison between our compounds, we started with suspensions with an amphiphile molarity of 10-4 Mol/L and SWNTs concentration of 0.01 g/L. Details on the synthesis of our compound can be found in the supporting information of our past publications [9], [10]. The used SWNTs are CoMoCATs nanotubes, purchased from SWeNTs and belonging to the SG76 batch. The suspensions were tip-sonicated for one hour at 60 W and centrifuged for another hour at 31000 g at room temperature. For the preparation steps, we used a Bandelin Sonopuls HD 2070 sonicator and a Hettig Mikro 220 R centrifuge.

The resulting supernatant was then collected and used for the spectroscopic characterization. Excitation photoluminescence characterization of the samples has been performed with a Nanolog spectrofluorometer from Horiba, equipped with a Xenon lamp and a liquid-Nitrogen cooled InGaAs detector. The absorption spectra have been acquired through a Perkin-Elmer Lambda 950 spectrophotometer.

3. Experimental results and discussion

Excitation photoluminescence (PLE) is a powerful technique to gain insight into the state of SWNTs in suspension. Each of the characteristic spots of such a map is univocally associated with a certain (n_1,n_2) chiral species and it occurs only if the tubes are isolated and as-pristine, undamaged by the functionalization process [18,19]. The emission intensity can thus be used to count the amount of pristine, isolated tubes in the suspensions [20]. The relative position of each spot in such charts is moreover sensitive to the environment and can be used to sense the strength and nature of interaction between the tubes and their surrounding:

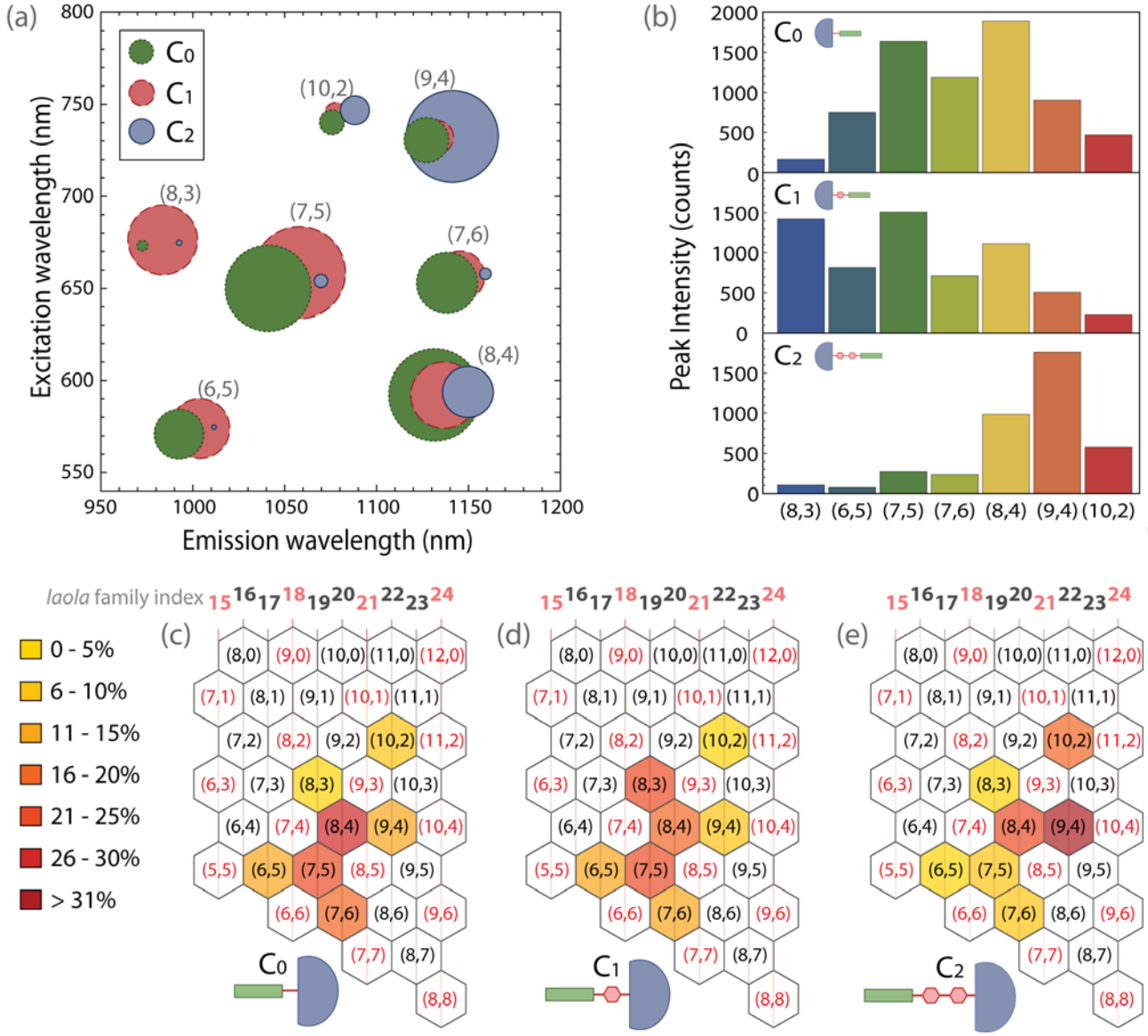

Figure 2 (a) Pseudo-PLE map of SWNTs functionalized with C_0 (green circles, dotted contour), with C_1 (red circles, dashed contour), and with C_2 (blue circles, solid contour). The radius of the circles is proportional to the intensity of the emitted band. **(b)** Intensity of the emission of our tubes coated with C_0 (upper panel), C_1 (central panel), and C_2 (lower panel). **(c)**, **(d)**, and **(e)** Hamada plots showing the distribution of the emission intensities between the chiral species coated, respectively, with C_0, C_1, and C_2. At the top of each plot are listed the *laola* family indexes.

Dielectric screening of the excitons cause shift of the emission and excitation features of the tubes with respect to their vacuum position [21]. Choi and Strano found that the intensity of the solvatochromic shifts scales as

$$Eii2\ \Delta Eii = c\ d^{-4}\ , \qquad (1)$$

where d is the nanotube diameter and, respectively, E_{11} is the energy of the emitted and E_{22} of the absorbed photons [22]. The slope c comprises information about the dielectric environment and it can be used to compare the strength of the effect of different dielectric environments on the tubes' features.

In Fig. 2(a) the positions of the emission bands of the carbon nanotubes coated with the different surfactants are disclosed. For each tube, the spots position changes with the molecule used for the coverage. The shifts are not rigid but change for different tube and different amphiphiles, indicating that each interacts distinctively with the different chiral species. The most striking peculiarity of our amphiphiles resides in the ability to disperse preferentially tubes belonging to distinct species. The distribution of the intensity of the radiation emitted by our samples is documented in Fig. 2(b). The heterogeneity of the distribution of the solubilized species can be appreciated also in Fig. 2(c), (d) and (e), where we compare the Hamada plots of the dispersions obtained through compounds C_0, C_1, and C_2. Increasing the number of phenyl rings comprised between head and tail, the most abundant chiral species in our suspensions are the ones belonging to laola families with increasing $2n_1+n_2$ family index (in bold in Fig. 2c,d,e).

Figure 3 compares the values of the slopes of the solvatochromic shifts calculated after the Choi and Strano model: The slopes of our compounds are bigger than the one of the commercially available reference SDS surfactant [22], indicating a bigger effect on the tubes than for SDS. We,

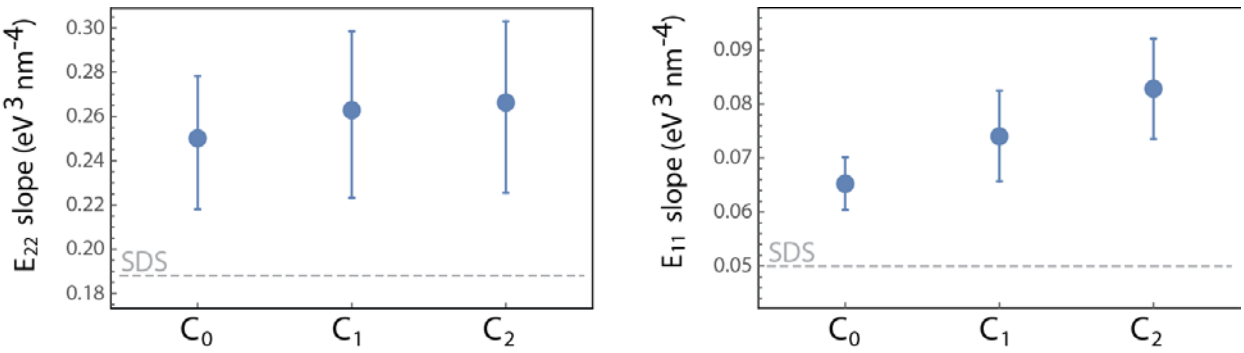

Figure 3 Slope of the solvatochromic shifts due to our amphiphiles. The dashed lines account for the values of the commercially available SDS reference surfactant [22].

moreover, observed a systematic uprise by increasing the amount of phenyl rings within the amphiphile core.

It is worth noting that the PLE technique is a very powerful technique to count the amount of isolated and as-pristine tubes available within a suspension. Nevertheless, PLE does not count all the tubes present within a sample, in particular tubes within small bundles that could be in suspension even after the sonication and that do not emit due to intra-bundle quenching mechanisms. Absorption spectroscopy, on the contrary, does not rely on emission of the tubes; its insensitivity to the bundling state makes it useful for counting the total amount of tubes within a sample. This is a very crucial aspect to be taken to consideration for separation. When comparing the performances of a surfactant, we need to verify its ability to solubilizes and isolate certain chiral species. PLE selectively detects only isolated tubes, absorption spectroscopy needs thus to be performed to cross-check and validate its results and exclude, for example, that other chiral species are present in the samples within bundles. In Fig. 4 we compare the absorption spectra of our suspensions. The spectra (grey dashed lines) have been fitted with Peak-o-Mat [23]. The fitted absorption bands are highlighted in the graphs. The S22(A) is mainly generated by the (6,5) and (8,4) species, the S22(B) from the (8,3), (7,5), and (7,6), and the S22(C) from the (9,4) and (10,2) species. The S11(A) is moreover indicating the presence of the (8,3) and (6,5) species, the S11(B)

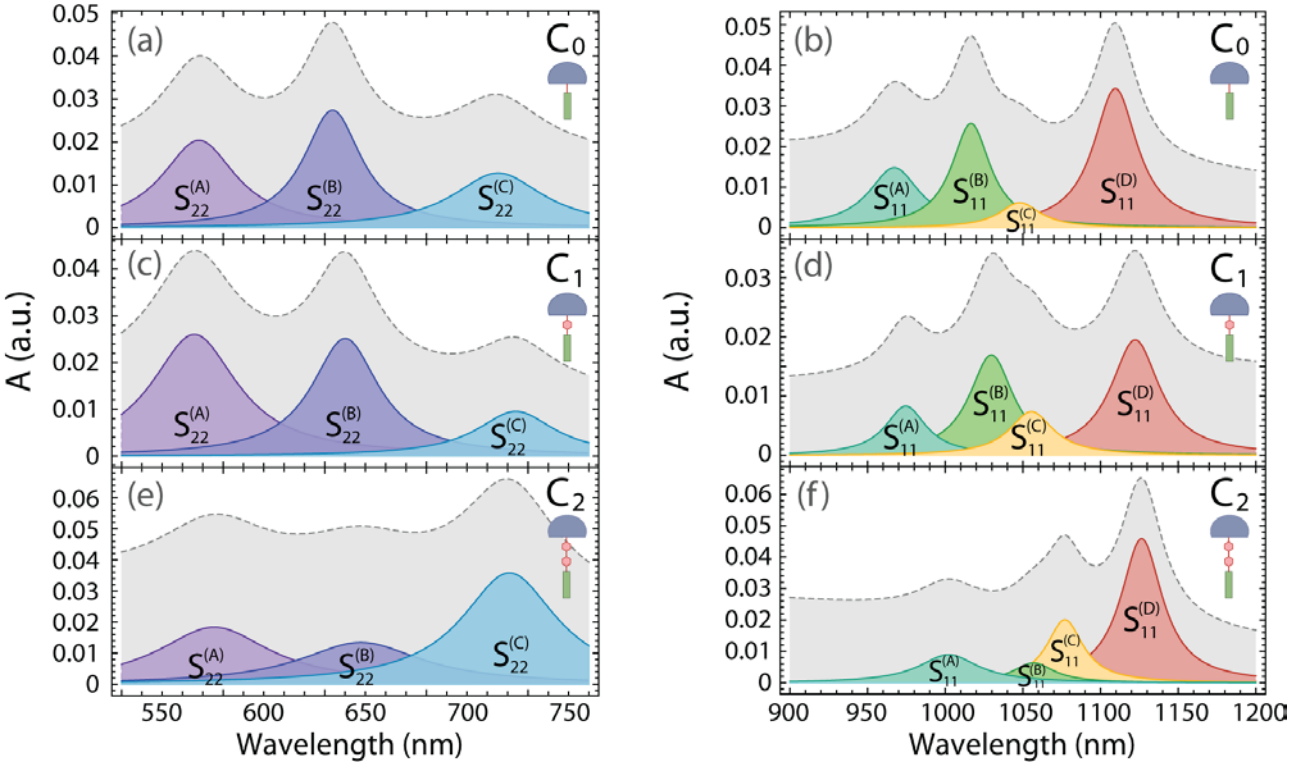

Figure 4(a), (c), (e) Absorption spectra in the E_{22} spectral region of the samples solubilized, respectively, with compounds C_0, C_1, and C_2. **(b), (d), (f)** Absorption spectra in the E_{11} spectral region of the samples solubilized, respectively, with compounds C_0, C_1, and C_2.

the (7,5) species, the S11(C) the (10,2) species, and the S11(D) the (9,4), the (7,6), and the (8,4) species. The absorption spectra already confirm the trends shown by the PLE spectra, with big changes in the composition of the suspensions between the different amphiphiles: The most dominant chiralities solubilized by compound C_0 and C_1 are the ones with the smaller family index, while the compound C_2 prefers solubilizing nanotubes with higher family index. It is worth noting that this analysis pertains semiconducting tubes only, while resonant Raman studies should be performed to cover the response of metallic species. Morphological studies of the micellar structures are to be performed to rationalize the correlation between amphiphile structure and resulting micelle property. Mastering the correlation between the core of our surfactants and the resulting structure they self-assemble into would help setting up a database of molecule of the isolation and transport of targeted nanotube species.

4. Conclusions

We showed that the rational design of surfactants with the same head and tail and comprising different small aromatic cores deeply influences the distribution of the different chiral species that end up isolated in solution. This results could be exploited for improving the efficiency of the single chirality selection at the solubilisation stage and encourage the further investigation of surfactants comprising other aromatic cores with different symmetries.

Acknowledgements

This work has been supported by the DFG under the SfB 658. A.S. gratefully thanks the FU Focus Area NanoScale for financial support.

References

[1] S. Reich, C. Thomsen, and J. Maultzsch, Carbon Nanotubes: Basic Concepts and Physical Properties (Wiley-VCH Verlag, Weinheim, 2004).

[2] J.R. Sachez-Valencia, T. Dienel, O. Gröning, I. Shorubalko, A. Mueller, M. Jansen, K. Amsharov, P. Ruffieux, and R. Fasel, Nature 512, 61 (2014).

[3] M. S. Arnold, A. A. Green, J. F. Hulvat, S. I. Stupp, and M. C. Hersam, Nature Nanotechnol. 1, 60 (2006).

[4] R. Krupke, F. Hennrich, H. von Loehneysen, and M. M. Kappes, Science 301, 344 (2003).

[5] T. Tanaka, H. Liu, S. Fujii, and H. Kataura, Phys. Status Sol-idi RRL 5, 301 (2011).

[6] C.Y. Khiripin, J.A. Fagan, and M. Zheng, JACS 135, 6822 (2013).

[7] R. Marquis, C. Greco, I. Sadokierska, S. Lebedkin, M.M. Kappes, T. Michel, L. Alvarez, J.L. Sauvajol, S. Meunier, and C. Mioskowski, Nano Letters 8, 1830 (2008).

[8] X. Tu, S. Manohar, A. Jagota, and M. Zheng, Nature 460, 250 (2009).

[9] A. Setaro, C.S. Popeney, B. Trappmann, V. Datsyuk, R. Haag, and S. Reich, Chem. Phys. Letters 493, 147 (2010).

[10] C.S. Popeney, A. Setaro, R.C. Mutihac, P. Bluemmel, B. Trappmann, J. Vonneman, S. Reich, and R. Haag, Chem. Phys. Chem. 13, 2013 (2012).

[11] P. Bluemmel, A. Setaro, C.S. Popeney, R. Haag, and S. Reich, Phys. Status Solidi B 247, 2891 (2010).

[12] A. Setaro, P. Bluemmel, C. Maity, S. Hecht, and S. Reich Adv. Funct. Mat. 22, 2425 (2012).

[13] F. Ernst, T. Heek, A. Setaro, R. Haag , and S. Reich, Journ. Phys. Chem. C 117, 1157, (2013).

[14] A. Setaro, C.S. Popeney, B. Trappmann, V. Datsyuk, R. Haag, and S. Reich, Phys. Status Solidi B 247, 2758 (2010).

[15] P. Bluemmel, A. Setaro, C.S. Popeney, B. Trappmann, R Haag, and S. Reich, Phys. Status Solidi B 248, 2532 (2011).

[16] C Kördel, A Setaro, P Bluemmel, CS Popeney, S Reich, and R Haag, Nanoscale 4, 3029 (2012).

[17] J. Yoo, H. Ozawa, T. Fujigaya, and N. Nakashima, Na-noscale 3, 2517 (2011).

[18] M.J. O'Connell, S.M. Bachilo, C.B. Huffman, et al. Science 297, 593 (2002).

[19] M.S. Strano, C.A. Dyke, M.L. Usrey, et al. Science 301, 1519 (2003).

[20] S. Heeg, E. Malic, C. Casiraghi, and S. Reich, Phys. Status Solidi B 246, 2740 (2009).

[21] C. Roquelet, J.-S. Lauret, V. Alain-Rizzo, C. Voisin, R. Fleurier, M. Delarue, D. Garrot, A. Loiseau, P. Roussignol, J.A. Delaire, and E. Deleporte, Chem. Phys. Chem. 11, 1667 (2010).

[22] J.H. Choi, M.S. Strano, Appl. Phys. Lett. 90, 223114 (2007).

[23] Peak-o-Mat is publicly available at the developer's web-site http://lorentz.sourceforge.net/.